Immunology
The Journal of cells, molecules, systems and technologies

British Society for immunology

IMMUNOLOGY ORIGINAL ARTICLE

Anti-tumour synergy of cytotoxic chemotherapy and anti-CD40 plus CpG-ODN immunotherapy through repolarization of tumour-associated macrophages

Ilia N. Buhtoiarov,[1,2] Paul M. Sondel,[1,2,3] Jon M. Wigginton,[4,*] Tatiana N. Buhtoiarova,[1] Eric M. Yanke,[1] David A. Mahvi[1] and Alexander L. Rakhmilevich[1,2]

[1]*Department of Human Oncology, University of Wisconsin, Madison, WI,* [2]*UW Paul P. Carbone Comprehensive Cancer Center, University of Wisconsin, Madison, WI,* [3]*Department of Pediatrics, University of Wisconsin, Madison, WI, and* [4]*Pediatric Oncology Branch, Center for Cancer Research, NCI At Frederick, Frederick, MD, USA*

doi:10.1111/j.1365-2567.2010.03357.x
Received 9 June 2010; revised 9 August 2010; accepted 18 August 2010.
*Present address: Jon M. Wigginton, Discovery Medicine-Clinical Oncology, Bristol-Myers Squibb, Inc., Princeton, NJ, USA.
Correspondence: A. L. Rakhmilevich, University of Wisconsin-Madison 4136 WIMR, 1111 Highland Avenue, Madison, WI 53705-2275, USA. Email: rakhmil@humonc.wisc.edu
Senior author: Alexander L. Rakhmilevich

Summary

We studied the effectiveness of monoclonal anti-CD40 + cytosine–phosphate–guanosine-containing oligodeoxynucleotide 1826 (CpG-ODN) immunotherapy (IT) in mice treated with multidrug chemotherapy (CT) consisting of vincristine, cyclophosphamide and doxorubicin. Combining CT with IT led to synergistic anti-tumour effects in C57BL/6 mice with established B16 melanoma or 9464D neuroblastoma. CT suppressed the functions of T cells and natural killer (NK) cells, but primed naïve peritoneal macrophages (Mϕ) to *in vitro* stimulation with lipopolysaccharide (LPS), resulting in augmented nitric oxide (NO) production. IT, given after CT, did not restore the responsiveness of T cells and NK cells, but further activated Mϕ to secrete NO, interferon-γ (IFN-γ) and interleukin (IL)-12p40 and to suppress the proliferation of tumour cells *in vitro*. These functional changes were accompanied by immunophenotype alterations on Mϕ, including the up-regulation of Gr-1. $CD11b^+$ $F4/80^+$ Mϕ comprised the major population of B16 tumour-infiltrating leucocytes. CT + IT treatment up-regulated molecules associated with the M1 effector Mϕ phenotype [CD40, CD80, CD86, major histocompatibility complex (MHC) class II, IFN-γ, tumour necrosis factor-α (TNF-α) and IL-12] and down-regulated molecules associated with the M2 inhibitory Mϕ phenotype (IL-4Rα, B7-H1, IL-4 and IL-10) on the tumour-associated Mϕ compared with untreated controls. Together, the results show that CT and anti-CD40 + CpG-ODN IT synergize in the induction of anti-tumour effects which are associated with the phenotypic repolarization of tumour-associated Mϕ.

Keywords: anti-CD40; chemotherapy; CpG-ODN; immunotherapy; monocytes/macrophages; tumour recognition

Introduction

Current cancer treatment frequently involves multiple treatment modalities, including surgery, radiation therapy, chemotherapy (CT) and immunotherapy (IT). The combination of several anti-tumour treatments (e.g. multiple distinct classes of chemotherapy) is more effective than monotherapy because they act on the tumour at multiple sites and via different mechanisms. However, multidrug CT regimens might be expected to interfere with immune-based therapies that depend on the actions of T cells and natural killer (NK) cells that are susceptible to CT-induced immune suppression.[1–7] We hypothesized that macrophages (Mϕ) might be more resistant to CT than other immune cells, and that IT directed towards the activation of Mϕ might therefore be synergistic with CT.

We recently established a preclinical IT protocol in tumour-bearing mice that was effective in suppressing tumour growth, even in the setting of profound immune deficiency, via the activation of Mϕ. This regimen combines agonistic monoclonal anti-CD40 and class B cytosine–phosphate–guanosine-containing oligodeoxynucleotide 1826 (CpG-ODN). This IT protocol was effective in controlling the growth of several distinct syngeneic murine tumours.[8] Anti-tumour effects were seen against B16

melanoma and NXS2 neuroblastoma (NB), neither of which express receptors for anti-CD40 (CD40) or CpG-ODN (TLR9),[8] as well as against CD40/TLR9-expressing B-cell chronic lymphoma.[9] In all models tested, the *in vivo* effect was mediated by Mϕ and did not appear to involve any direct cytotoxic/pro-apoptotic effect of anti-CD40 or CpG-ODN. These preclinical results may have clinical relevance as Mϕ comprise a major population of tumour-infiltrating leucocytes in many types of cancer.[10,11]

Multidrug CT protocols, such as VCD (vincristine + cyclophosphamide + doxorubicin), are commonly used clinically for the treatment of solid and haematological malignancies[12–14] and are also known for their immunosuppressive effects against lymphoid cells.[15] In this study we tested if combining the VCD CT regimen with anti-CD40/CpG-ODN IT would result in augmented anti-tumour effects in immunocompetent C57BL/6 mice. It was found that these CT and IT regimens synergized in inducing anti-tumour effects *in vivo* despite CT-induced suppression of effector functions of T cells and NK cells. Further analyses demonstrated that CT primed Mϕ to subsequent stimulation via CD40 and TLR9 that resulted in augmented Mϕ secretory and anti-tumour properties *in vitro*. Analyses of tumour-associated Mϕ (TAM) from CT plus IT-treated tumour-bearing mice revealed that *in vivo* anti-tumour effects were paralleled by the changing of TAM from a pro-tumour (M2) phenotype into Mϕ with an effector (M1) phenotype.

Materials and methods

Mice

Six- to ten-week-old C57BL/6 mice (Harlan Sprague Dawley, Madison, WI), were housed, cared for and used in accordance with the *Guide for Care and Use of Laboratory Animals* (NIH publication 86-23, National Institutes of Health, Bethesda, MD, 1985).

Tumour cell lines

Mouse B16 melanoma and 9464D NB cell lines were grown in complete RPMI-1640 or Dulbecco's modified Eagle's minimal essential medium (DMEM), respectively, supplemented with 10% fetal bovine serum (FBS) (Sigma-Aldrich, St Louis, MO), 2 mM L-glutamine, 100 U/ml of penicillin/streptomycin and 0·5 μM 2-mercaptoethanol (2-ME) (Invitrogen Life Technologies, Carlsbad, CA) at 37° in a humidified 5% CO_2 atmosphere. The 9464D disialoganglioside-2-positive, *N-myc*-overexpressing NB cell line was established in the laboratory of Dr Jon Wigginton (NCI), and was derived from spontaneous NB tumours arising in C57BL/6 *N-myc* transgenic mice developed originally by Dr William A. **Weiss** (University of California, San Francisco, CA).[16]

In vivo *tumour models and measurement of anti-tumour effects*

Subcutaneous B16 melanoma and 9464D NB tumours were established by the injection of 1×10^5 B16 cells/0·05 ml and 2×10^6 9464D cells/0·1 ml phosphatebuffered saline (PBS) in the abdomen. Anti-tumour effects were evaluated by measuring *in situ* tumour volumes, calculated as follows: smaller diameter (mm) × smaller diameter (mm) × larger diameter (mm) × (π/6), and expressed as mean ± standard error of the mean (SEM) of tumour sizes of all mice of the experimental group.

Intra-adrenal 9464D tumours were established by direct implantation of 1×10^6 tumour cells in 0·03 ml PBS into the left adrenal gland, as previously described.[17] Anti-tumour effects were evaluated by measuring the perpendicular sizes of the excised tumour, calculated as follows: smaller diameter (mm) × smaller diameter (mm) × larger diameter (mm) × (π/6), and expressed as mean ± SEM of tumour sizes of all mice of the treatment group. Alternatively, excised peri-renal tumour masses were weighed and the weight of the contralateral normal kidney was subtracted to yield the net tumour weight, which was expressed as mean ± SEM of the net tumour weights of all mice of the experimental group.

CT and IT protocols

CT treatment group Naïve or tumour-bearing mice were treated with VCD CT (vincristine 0·5 mg/kg, cyclophosphamide 100 mg/kg, doxorubicin 3·3 mg/kg)[18] via a single injection in a total volume of 0·25 ml of PBS. Administration was either intraperitoneal or intravenous, and is specified for each experiment. For naïve mice, CT treatment was performed on day 0, followed by 0·25-ml injections of PBS on days 3 and 6 as control treatments for IT. For tumour-bearing mice the treatment was usually started on days 8–10 after tumour implantation, unless specified otherwise for certain experiments.

IT treatment group Monoclonal anti-CD40 was obtained from ascites of nude mice injected with FGK 45.5 hybridoma cells (a gift from Dr F. Melchers, Basel Institute for Immunology, Basel, Switzerland) and enriched for IgG by ammonium sulphate precipitation. Endotoxin-free CpG1826 (TCCATGACGTTCCTGACGTT; the CpG motifs are underlined) was purchased from Coley Pharmaceuticals Group (Wellesley, MA). Administration was either intraperitoneal. or intravenous, and is specified for each experiment. Naïve mice were treated with agonistic anti-CD40 (0·5 mg/0·25 ml, unless indicated otherwise)

on day 3 and CpG-ODN 1826 (0·1 mg/0·25 ml, unless indicated otherwise) on day 6, with these two treatments preceded by injection of 0·25 ml of PBS on day 0 as a control treatment for CT (see above). For tumour-bearing mice the treatment was usually started on days 8–10 after tumour implantation, unless specified otherwise for certain experiments.

CT + IT In experimental groups where CT and IT were combined, anti-CD40 was given 3 days after CT, and CpG-ODN was given 3 days after treatment with anti-CD40. Control groups received PBS. In some experiments, the CT + IT cycles were repeated, with 3–4 days of rest between cycles.

Splenocyte preparation Splenocytes were prepared from whole spleens pooled from three C57BL/6 mice by processing the spleens to a single-cell suspension, followed by lysis of erythrocytes by hypotonic shock.

Splenic T-cell proliferation assay Flat-bottom 96-microwell cell-culture clusters were precoated with 5 μg/ml (0·1 ml/well) of monoclonal anti-CD3 (clone 145-2C11, functional grade purified hamster IgG) or control hamster IgG, both from eBioscience (San Diego, CA), for 24 hr at 4°, and the unbound IgG was removed by washing with ice-cold PBS.

Before plating, the splenocyte preparations from different treatment groups were analyzed by flow cytometry to determine the number of $CD3^+$ cells, and the samples were adjusted to 5×10^5 $CD3^+$ T cells/ml. Fifty-thousand $CD3^+$ cells were cultured in triplicate for 72 hr in complete medium in plates precoated with anti-CD3- or control IgG. To measure cell proliferation, the cells were pulsed with 1 μCi/well of [^{3}H]thymidine ([^{3}H]TdR) for the last 6 hr, and retained radioactivity was counted by β-scintillation of total cells harvested from the wells onto glass fibre filters (Packard Instrument, Meriden, CT), using the Packard Matrix 9600 Direct Beta Counter (Packard Instrument). The results represent the mean ± SEM of β-scintillation counts acquired in 5 min from triplicate samples.

Splenic NK cell-medicated cytotoxicity Splenocytes from mice of different treatment groups were adjusted to 1×10^5 $Ly49b^+$ NK cells/ml and cultured in medium supplemented with 100 U/ml of recombinant human interleukin (IL)-2. At 72 hr of culture, the cells were harvested and readjusted to 5×10^5 viable total splenocytes/0·1 ml, and thereafter tested for lysis of 5×10^3 NK cell-sensitive ^{51}Cr-pulsed YAC-1 cells at different effector-to-target (E/T) ratios (100:1, 50:1, 25:1, 12·5:1) following 4 hr of co-culture in a final volume of 0·2 ml. After 4 hr of incubation, the supernatant was harvested utilizing the Skatron harvesting system (Skatron, McLean, VA) and cytotoxicity values (%) were calculated at each E/T ratio, as reported previously.[19]

In vitro *Mϕ-mediated inhibition of tumour cell proliferation* Peritoneal cells (PCs) were obtained from mice by peritoneal cavity lavage. Before plating, PCs from different treatment groups were analyzed by flow cytometry to determine the proportion of $CD11b^+$ $F4/80^+$ cells, and thereafter seeded in 96-microwell flat-bottom cell-culture clusters at $2{\cdot}5–3 \times 10^5$ $CD11b^+$ $F4/80^+$ cells/0·2 ml. Ninety minutes later, non-adherent cells were removed from the culture by repeated pipetting. This protocol yields a relatively pure population of Mϕ, based on co-expression of F4/80 and CD11b on 97% of cells.[20] The resultant adherent Mϕ were thereafter incubated with B16 tumour cells (5×10^5 cells/ml, 0·05 ml/well, unless otherwise indicated) for 48 hr in medium with or without 10 ng/ml of lipopolysaccharide (LPS) from *Salmonella enteritidis* (Sigma-Aldrich) in a final volume of 0·2 ml.

To measure tumour cell proliferation, the cell cultures were pulsed with 1 μCi/well of [^{3}H]TdR for the last 6 hr, and retained radioactivity was counted by β-scintillation of total cells harvested from the wells onto glass fibre filters (Packard Instrument), using the Packard Matrix 9600 Direct Beta Counter (Packard Instrument). Under these conditions Mϕ incorporate negligible amounts of [^{3}H]TdR, enabling [^{3}H]TdR to reflect the level of proliferation of the tumour cells. Inhibition of proliferation was calculated as $c = [(a-b)/a] \times 100$, where c is the inhibition index; a is the mean value of [^{3}H]TdR incorporated into tumour cells cultured in triplicate in medium without Mϕ, in the absence or presence of LPS; and b is the mean value of [^{3}H]TdR incorporated into tumour cells cultured in triplicate in medium with Mϕ, in the absence or presence of LPS.

Nitric oxide detection Mϕ were cultured with tumour cells, as described above, to determine the inhibition, *in vitro*, of Mϕ-mediated tumour cell proliferation. At 48 hr of co-culture, the Mϕ-containing tumour cell culture supernatants were collected without disturbing the cell monolayers. Nitrite accumulation in the cell-culture supernatants was determined by using the Griess reagent (Sigma-Aldrich) as described previously.[21]

Labelling of PCs with carboxyfluoroscein succinimidyl ester Carboxyfluoroscein succinimidyl ester (CFSE: **excitation,** 490 nm; emission, 518 nm) was purchased from Invitrogen (Carlsbad, CA). Before labelling, PCs (pooled from 10–20 naïve C57BL/6 mice) were washed twice with PBS at room temperature to eliminate mouse serum residua, resuspended in 10 ml of 37° PBS supplemented with 5 mM of CFSE and incubated for 15 min at 37°. The PCs were washed once with ice-cold PBS containing 10% FCS (to neutralize free, cell-unbound label) and once with

serum-free PBS, resuspended at $2–4 \times 10^6$ PC/ml and injected intraperitoneally into mice.

Flow cytometry analysis

Phenotypic and quantitative analysis of splenocytes Splenocyte preparations were resuspended in ice-cold PBS + 2% FCS at 3×10^6 cells/ml, dispensed in flow cytometry testing Falcon tubes at 3×10^5 cells/0·1 ml and stained with 0·1 μg/sample of anti-CD3-conjugated fluorescein isothiocyanate (FITC) (clone 145-2C11), anti-B220–FITC (RA3-6B2), anti-CD11b–allophycocyanin (M1/70), anti-Ly49b–FITC (DX5), anti-F4/80–FITC (BM8) and anti-Gr1-conjugated phycoerythrin (PE) (RB6-8C5) all from eBioscience, for 40 min on ice, followed by cell washing with ice-cold PBS and fixation with 2% paraformaldehyde. Analysis of F4/80 (BM8) and Gr-1 (RB6-8C5) expression on splenic Mϕ was performed by gating on $CD11b^+$ cells. Data acquisition was performed on a FACSCalibur flow cytometer with CellQuest software (BD, Franklin Lakes, NJ). Analysis was performed on FlowJo (TreeStar, Inc., Ashland, OR) software. To calculate the absolute number of a splenocyte subset in the total pool of splenocytes, the absolute number of total splenocytes (obtained via counting the cells on a haemocytometer) was multiplied by the relative prevalence of that subset (%) obtained via flow cytometry analysis. The results were expressed as the absolute number ($\times 10^6$) of the population expressing the antigen of interest.

Phenotypic and quantitative analysis of Mϕ PCs were harvested and counterstained with anti-CD11b–allophycocyanin (M1/70), anti-F4/80–FITC (BM8), anti-Gr1–PE (RB6-8C5), anti-Ly6C-conjugated peridinin chlorophyll protein (PerCP)-Cy5.5 (HK1.4), all from eBioscience, and anti-Ly6G–PE (1A8), from BD Bioscience, on ice for 40 min, followed by repeated cell washing with ice-cold PBS + 2% FCS and fixation in 2% paraformaldehyde. Data acquisition was performed on a FACSCalibur flow cytometer with CellQuest (BD) software. Analyses were performed on FlowJo (Tree Star, Inc., Ashland, OR) software by gating on $CD11b^+$ $F4/80^+$ cells.

In separate experiments, collected PCs were seeded in six-well plates at 1×10^6 PC/ml, 5 ml, with subsequent removal of non-adherent cells, and were thereafter cultured for 12 hr in complete medium supplemented with 10 ng/ml of LPS and 1 μM monensin. At 12 hr of culture, the adhesion-purified Mϕ were harvested with 0·53 mM EDTA, resuspended in PBS + 2% FCS, then stained with anti-CD11b–allophycocyanin and F4/80–FITC for 40 min on ice. After staining with anti-CD11b/F4/80–allophycocyanin, the cells were washed in ice-cold PBS, fixed and permeabilized as previously described,[8] and stained with anti-interferon-γ (IFN-γ)–PE (XMG1.2) and anti-IL-12–PE (C17.8). Flow cytometry analysis was performed as described above. The results are presented as mean fluorescence intensity (MFI) ratios, calculated as the value of MFI of staining with a specific monoclonal antibody (mAb) divided by the value of MFI of staining with isotype-matched control IgG; the MFI ratio equals 1 when an antigen is not expressed. This approach allows for comparison of the same parameter but in different experimental conditions. Quantitative analysis of $CD11b^+$ $F4/80^+$ PCs was performed as described above for the analysis of $CD11b^+$ splenic Mϕ.

Analysis of tumour-associated Mϕ Harvested subcutaneous tumours were mechanically disaggregated and single-cell suspensions were obtained by centrifugation through a Ficoll–Paque density gradient at 450 ***g*** using a GH-3.8 rotor for 30 min. The tumour-cell preparations were resuspended in ice-cold PBS + 2% FCS at 5×10^6 total cells/ml, dispensed in flow cytometry testing Falcon tubes at 5×10^5 cells/0·1 ml and stained with 0·1 μg/sample of anti-CD45–allophycocyanin (30-F1), anti-CD11b–FITC or –allophycocyanin (M1/70), anti-F4/80–FITC (BM8), anti-Gr1–PE (RB6-8C5), anti-CD40–PE (1C10), anti-MHC class II–PE (M5/114.15.2), anti-CD80–PE (16-10A1), anti-CD86–PE (GL1) and anti-Ly6C–PerCP-PECy5.5 (HK1.4), all from eBioscience, and anti-Ly6G–PE (1A8), anti-IL-4R-alpha–PE (mIL4R-M1), anti-B7-H1–PE (MIH5), from BD Bioscience, for 40 min on ice, followed by repeated cell washing with ice-cold PBS + 2% FCS and fixation in 2% paraformaldehyde. Analysis was performed, as described above, by gating on $CD45^+$ $CD11b^+$ tumour-infiltrating leucocytes or $CD11b^+$ $F4/80^+$ Mϕ.

Alternatively, tumour-derived single-cell preparations were plated in six macro-well cell-culture clusters at 5×10^6 total cells/ml, in 5 ml, in complete RPMI-1640 supplemented with 1 mM monensin. At 12 hr the cells were harvested with 5% EDTA, resuspended in PBS + 2% FCS, then stained with anti-CD11b–allophycocyanin and anti-F4/80–FITC for 40 min on ice. Subsequently, the cells were washed in ice-cold PBS, fixed and permeabilized as previously described,[8] and stained with anti-IL-4–PE (11B11), anti-IL-10–PE (JES5-16E3), anti-IFN-γ–PE (XMG1.2), anti-tumour necrosis factor-α (TNF-α)–PE (MP6-XT22), or anti-IL-12–PE (C17.8). Flow cytometry analysis was performed, as described above, by gating on $CD11b^+$ $F4/80^+$ Mϕ. The results are presented as MFI ratios.

Statistical analysis A two-tailed Student's *t*-test was used to determine significant differences between experimental and relevant control values within one experiment. Statistical analysis of inhibition of the tumour cell proliferation under different experimental conditions was performed on original [^{3}H]TdR-incorporation values, which were also used to calculate the percentage of inhibition.

Results

VCD-CT and anti-CD40 + CpG-ODN IT synergize in inducing anti-tumour effects *in vivo*

We have previously shown that anti-CD40 and CpG-ODN synergize in activating Mϕ and suppressing the growth of tumours in various models.[8,9] As Mϕ are relatively resistant to certain CT regimens,[22] we hypothesized that the anti-tumour effects induced by CT will be augmented by anti-CD40 and CpG-ODN IT. To determine the anti-tumour effect of CT alone, mice bearing palpable subcutaneous B16 tumours were given a single cycle of VCD-CT on days 3, 8 or 11 after the tumour had been implanted, and the tumour growth (Fig. 1a) and survival (Fig. 1b) were monitored. Significant suppression of tumour growth was seen when treatment was started on days 3 or 8. However, complete tumour resolution was not achieved, and survival of the mice was extended by less than twofold.

Next, we tested whether a combination of CT with IT would result in synergistic anti-tumour effects in mice bearing subcutaneous B16 tumours. CT was given on days 8 and 17 after tumour implantation, and anti-CD40 was given on days 11 and 20 followed by CpG-ODN 3 days later[8] (i.e. on days 14 and 23). Animals that received both CT and IT showed the strongest anti-tumour response, resulting in significant inhibition of tumour growth ($P < 0{\cdot}001$, CT + IT versus CT or IT alone, Fig. 1c). In addition, the tumours in the CT + IT group showed transient shrinkage of volume, with the tumours in this group being smaller on day 26 than on day 8 ($P = 0{\cdot}0002$). This combined treatment also resulted in significant (3·5-fold) prolongation of survival compared with other groups (Fig. 1d).

To confirm the synergy between CT and IT observed in this subcutaneous B16 tumour model, we delivered CT or IT, alone or in combination, to C57BL/6 mice bearing subcutaneous 9464D NB tumours (Fig. 1e,f). The combined CT + IT treatment resulted in very potent suppression of tumour growth (Fig. 1e) as well as significantly prolonged survival of the tumour-bearing mice compared with other groups (Fig. 1f).

The synergy between CT and IT was also seen when used to treat mice bearing intra-adrenal 9464D NB tumours. The CT and IT administered in combination induced the strongest anti-tumour effects based on tumour weight (Fig. 1g), tumour volume (Fig. 1h) and overall mouse survival (Fig. 1i; 33 days for the control group versus 69 ± 1·55 days for the CT + IT treatment group, $P < 0{\cdot}001$).

CT + IT treatment results in redistribution of major subsets of spleen leucocytes

CT is known to frequently cause temporary lymphocytopenia, whereas IT may result in the expansion of certain subsets of lymphocytes. We evaluated the total numbers of splenocytes as well as the total numbers of $CD3^+$ T cells, $B220^+$ B cells, $CD11b^+$ Mϕ and $Ly49b^+$ NK cells in the spleens of naïve mice after a single cycle of CT and IT, separately or in combination. As shown in Fig. 2, CT

Figure 1. Chemotherapy (CT) and immunotherapy (IT) synergize in inducing anti-tumour effects *in vivo*. (a,b) C57BL/6 mice ($n = 5$ per group) bearing subcutaneous B16 melanoma tumours were treated with CT, via a single intraperitoneal injection, on different days after tumour implantation. Tumour volumes, expressed as mean ± standard error of the mean (SEM), (a) and survival (b) were monitored. (a) $*P > 0{\cdot}05$ (control versus CT day 11); $@P < 0{\cdot}02$ (control group versus CT day 3 or CT day 8); $\#P > 0{\cdot}05$ (CT day 3 versus CT day 8). (b) $*P > 0{\cdot}05$ (control versus CT day 11); $@P = 0{\cdot}031$ (control group versus CT day 3); $\#P = 0{\cdot}043$ (control group versus CT day 8); $\&P > 0{\cdot}05$ (CT day 3 versus CT day 8). (c,d) C57BL/6 mice ($n = 6$ per group) bearing subcutaneous B16 melanoma tumours were treated intravenously with CT on days 8 and 17 after tumour implantation and IT (anti-CD40 on days 11 and 20 plus CpG-ODN 1826 on days 14 and 23 after tumour implantation), alone or in combination. Tumour volumes (c) and mouse survival (d) were monitored. (c) $*P < 0.001$ (control versus CT or IT); $@P < 0{\cdot}001$ (CT or IT versus CT + IT). (d) $*P > 0{\cdot}05$ (control versus CT); $@P = 0{\cdot}036$ (control versus IT); $\#P < 0{\cdot}01$ (control versus CT + IT); $\&P < 0{\cdot}02$ (CT + IT versus either CT or IT). (e,f) C57BL/6 mice ($n = 5$ per group) bearing subcutaneous 9464D neuroblastoma (NB) tumours were treated intraperitoneally with CT on day 15 after tumour implantation, and IT (anti-CD40 on days 18 and 25 plus CpG on days 21 and 28 after tumour implantation), alone or in combination. Tumour volumes (e) and mouse survival (f) were monitored. (e) $*P > 0{\cdot}05$ (control versus IT); $@P < 0{\cdot}006$ (control versus CT); $\#P < 0{\cdot}007$ (CT + IT versus CT or IT). (f) $*P > 0{\cdot}05$ (control versus IT); $@P < 0{\cdot}05$ (control versus CT); $\#P > 0{\cdot}05$ (CT versus IT); $\&P < 0{\cdot}03$ (control versus CT + IT); $\wedge P < 0{\cdot}05$ (CT + IT versus CT or IT). (g–i) C57BL/6 mice ($n = 9$ per group) bearing intra-adrenal 9464D NB tumours were treated with CT on days 10 and 20 after tumour implantation, and with IT (anti-CD40 on days 13 and 23 plus CpG on days 16 and 26 after tumour implantation), alone or in combination. Mice were monitored for tumour growth by left flank palpation every third day. On day 33 after tumour implantation, when animals of the control group showed symptoms as a result of the large tumour size, all mice of the control group and three randomly selected mice from each of the experimental groups were killed, and tumour weight (g) and volume (h) were calculated and compared with those in mice killed on day 10 after tumour implantation, before the treatment started. The rest of the treated animals were also followed for survival (i). (g) $*P = 0{\cdot}0027$, $@P = 0{\cdot}0307$, $\#P = 0{\cdot}002$, $\&P = 0{\cdot}0001$, $\wedge P = 0{\cdot}0046$. (h) $*P = 0{\cdot}0013$, $@P = 0{\cdot}0307$, $\#P = 0{\cdot}015$, $\&P = 0{\cdot}009$, $\wedge P = 0{\cdot}017$. (i) $*P = 0{\cdot}027$ (control versus IT); $@P = 0{\cdot}009$ (control versus CT); $\#P = 0{\cdot}041$ (CT versus IT); $\&P < 0{\cdot}001$ (control versus CT + IT); $\wedge P < 0{\cdot}025$ (CT + IT versus CT or IT). Presented are the results from one experiment (a,b), and representative of three experiments (c,d) or two experiments (e,f and g,i). D3, day 3; D8, day 8; D11, day 11.

caused a statistically significant decrease in the numbers of total splenocytes (Fig. 2a) because of a reduction, at least in part, of the total number of B cells and NK cells (Fig. 2b). In contrast, IT resulted in increased numbers of all four subsets of splenic cells. When IT was administered after CT, it did not significantly change the number of total splenocytes compared with CT alone (Fig. 2a), but led to an increase in the overall number of $CD11b^+$ splenic Mϕ (*$P = 0{\cdot}022$) while decreasing the numbers of T cells, B cells and NK cells (Fig. 2b).

A number of cells are known to express CD11b (also known as integrin alpha M antigen, macrophage-1 alpha antigen, or complement receptor-3): monocytes, Mϕ and microglia express high levels of CD11b, whereas granulocytes, NK cells, $CD5^+$ B-1 cells and certain subsets of dendritic cells express CD11b to a much lower extent. Recent analyses of naïve and tumour-bearing mice have identified populations of $CD11b^+$ cells with varying levels of Gr-1 expression and co-expression of F4/80; their suppressive activity has been used to characterize them as myeloid-derived suppressor cells (MDSCs), but not all cells with these markers are suppressive. We evaluated the $CD11b^{high}$ splenocytes (Fig. 2ci, region G) for co-expression of F4/80 (a pan-Mϕ marker) as well as Gr-1 (the

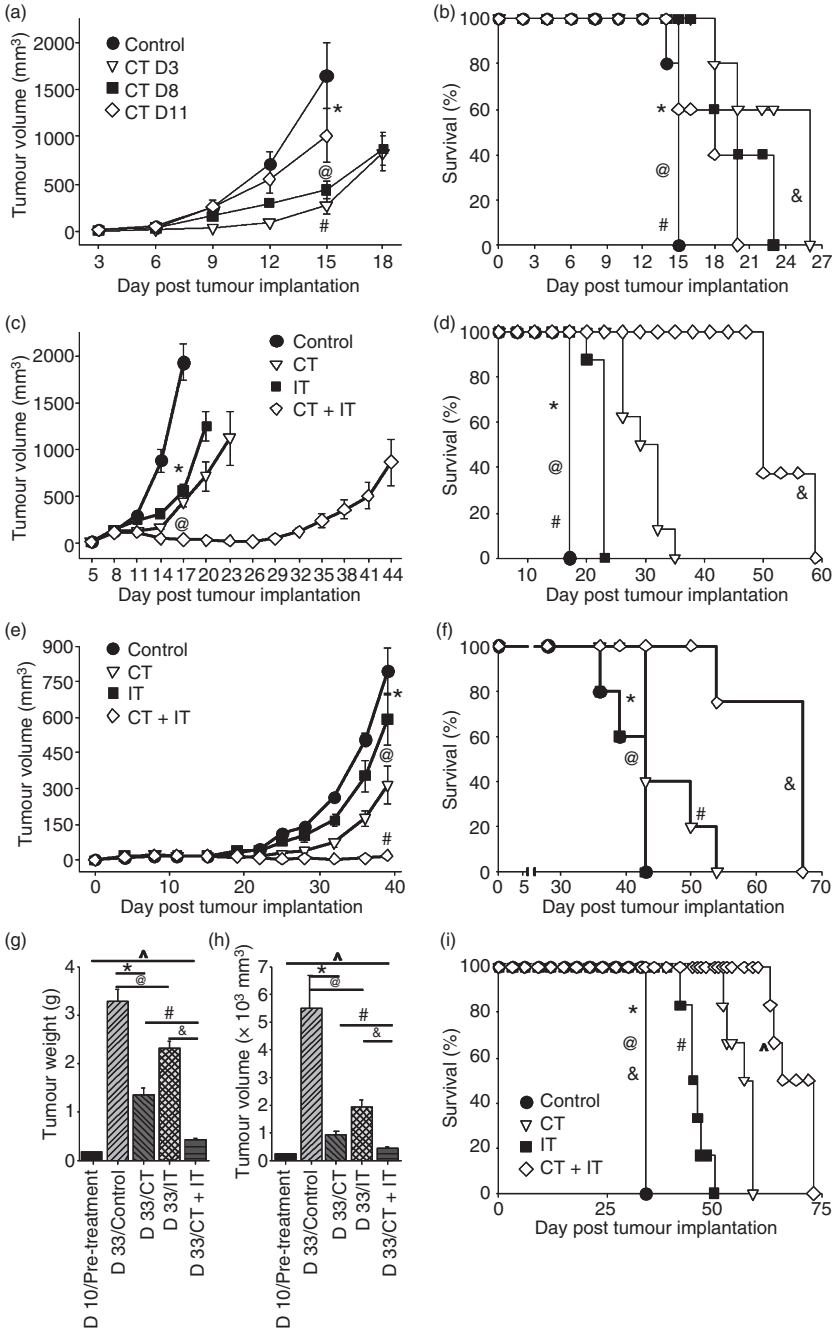

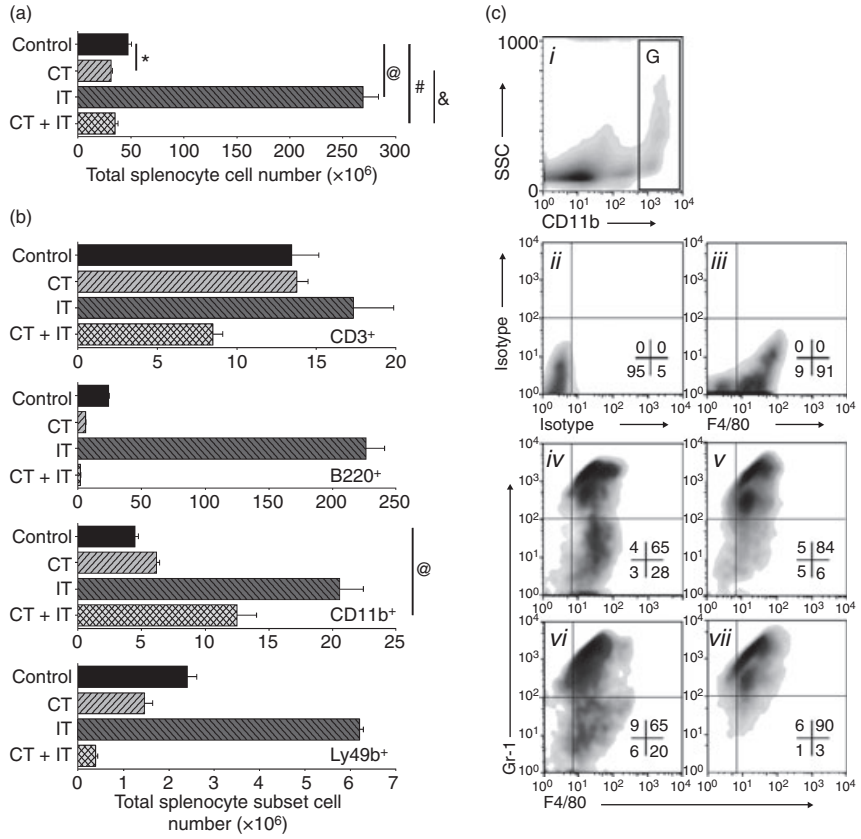

Figure 2. Differential leucodepletion effect of chemotherapy (CT) on splenic T cells, B cells, natural killer (NK) cells and macrophages (Mϕ). Naïve non-tumour-bearing C57BL/6 mice ($n = 4$ per group) were treated (intraperitoneally or intravenously in several different experiments) with CT or immunotherapy (IT), alone or in combination, as described in the Materials and methods, and spleens were harvested on day 7 [i.e. one day after the last treatment; the second injection of phosphate-buffered saline (PBS) for the CT-treatment group, or CpG-ODN for IT and CT + IT treatment groups]. Absolute numbers of total splenocytes (a) or splenic $CD3^+$ T cells, $B220^+$ B cells, $CD11b^+$ Mϕ and $Ly49^+$ NK cells (b) were computed based on the total number of cells and cell subset percentages from the flow cytometric analyses. The results are representative of at least three separate experiments. (a) $*P = 0{\cdot}0112$, $@P = 0{\cdot}0001$, $\#P = 0{\cdot}464$, $\&P = 0{\cdot}3351$. (b) ($CD11b^+$) $P = 0{\cdot}022$. (c) Splenic cells from mice receiving the treatments indicated below were gated on $CD11b^{high}$ cells [region (g) in panel ci for control mice] and analyzed for expression of F4/80 and Gr-1 (ciii–cvii). Panel cii shows the isotype-control staining, in place of the anti-F4/80 and anti-Gr-1. Panel ciii shows staining with anti-F/80 and isotype (for anti-Gr-1) monoclonal antibodies (mAbs). Panels iv–vii show staining with anti-F4/80 and anti-Gr-1 of Mϕ from mice treated with vehicles (iv), CT (v), IT (vi) and CT + IT (vii). Numbers in density plots indicate the percentage of events in each quadrant. Data are representative of at least three experiments, with similar results obtained in each.

myeloid differentiation antigen) (Fig. 2cii–vii). It was found that the $CD11b^{bright}$ splenocyte population is represented by two distinct subsets: a major subset of $F4/80^+GR\text{-}1^{bright}$ cells and a minor subset of $F4/80^+$ $GR\text{-}1^{dim}$ cells (Fig. 2civ–vii). Interestingly, CT (Fig. 2cv), alone or in combination with IT (Fig. 2cvii), increased the prevalence of $F4/80^+$ $GR\text{-}1^{bright}$ cells; ~96% of all $CD11b^{bright}$ splenocytes in mice receiving the combined CT+IT treatment were also $Gr\text{-}1^{bright}$ (Fig. 2cvii).

CT treatment results in differential immunosuppression

Having documented quantitative changes in the composition of the splenic cell subset after treatment with CT, alone, or in combination with IT (Fig. 2), we then investigated whether this VCD-CT regimen, with or without IT, could affect the functional characteristics of the major immune effectors involved in anti-tumour responses (Fig. 3a–e). First, we tested splenic $CD3^+$ T cells for their ability to proliferate in response to *in vitro* stimulation with plate-bound anti-CD3 mAb (Fig. 3a). As shown, T cells from control and IT-treated animals proliferated well after CD3 stimulation. In contrast, splenocytes from the CT-treated group and from the CT + IT treatment group showed minimal proliferative response to the CD3 stimulation. Thus, CT induced profound T-cell suppression, and the IT failed to restore T-cell proliferative function.

Next, we tested the ability of splenic NK cells to lyse YAC-1 cells *in vitro* (Fig. 3b). As shown, splenic NK cells from the control and IT-treated groups efficiently lysed YAC-1 cells. In contrast, NK cells from mice that received

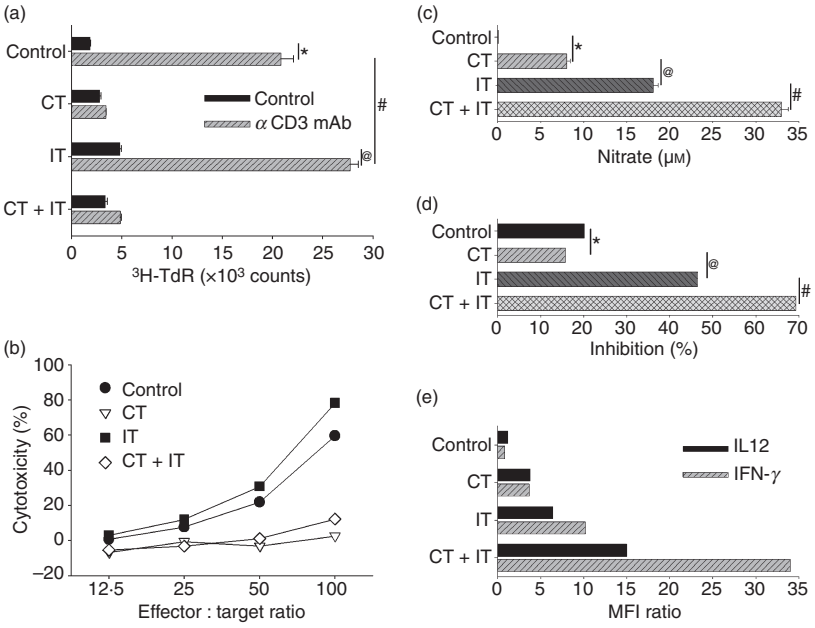

Figure 3. Differential effect of chemotherapy (CT) treatment on the functions of T cells, natural killer (NK) cells and macrophage (Mϕ). (a) Splenocytes from naïve (i.e. non-tumour-bearing) C57BL/6 mice ($n = 3$ per group) treated intraperitoneally with CT and immunotherapy (IT), alone or in combination, as described in the Materials and methods and in the legend for Fig. 2, were adjusted to 5×10^4 $CD3^+$ T cells/0·1 ml and cultured in 96-microwell tissue culture clusters precoated with αCD3 monoclonal antibody (mAb) or control IgG for 72 hr. Proliferation of splenocytes was measured by the incorporation of [^{3}H]thymidine during the last 6 hr of culture. *$P = 0·0001$, @$P = 0·0001$, #$P = 0·052$. (b) Splenocytes from mice ($n = 3$ per group) treated intraperitoneally with CT and IT, alone or in combination, were adjusted to 1×10^5/ml of $Ly49b^+$ NK cells and cultured in medium supplemented with 100 U/ml of recombinant human IL-2 for 72 hr. After this *in vitro* stimulation, the cell suspensions were readjusted to 5×10^5 viable total splenocytes/0·1 ml and tested for lysis of 5×10^3 NK cell-sensitive ^{51}Cr-labelled YAC-1 cells/0.1 ml at the indicated effector-to-target ratios following 4 hr of co-culture in a final volume of 0·2 ml. The results are presented as percentage of cytotoxicity. (c–d) Peritoneal cells (PC) from mice treated intraperitoneally with CT and IT, alone or in combination, were adjusted to $2·5 \times 10^5$ $CD11b^+$ $F4/80^+$ Mϕ/0·1 ml, seeded in 96-microwell clusters, purified for Mϕ by adhesion to plastic, and thereafter tested *in vitro* for nitric oxide (NO) production (c) and inhibition of B16 tumour cell proliferation following 48 hr of co-culture *in vitro* with 1×10^3 B16 tumour cells/0·1 ml in medium supplemented with 10 ng/ml of lipopolysaccharide (LPS) (d). (c) *$P = 0·01$, @$P = 0·006$, #$P = 0·002$. (d) *$P = 0·7$, @$P = 0·01$, #$P = 0·009$. (e) PC from CT and/or IT-treated mice ($n = 3$ per group) were purified for Mϕ by adhesion to plastic and cultured for 12 hr in medium supplemented with 1 μM monensin and 10 ng/ml of LPS, followed by flow cytometric assessment of the intracellular expression of IL-12 and IFN-γ. The results are presented as MFI ratios and are representative of at least three separate experiments with similar results obtained in each.

CT alone or in combination with IT mediated minimal cytotoxicity, even with *in vitro* IL-2 stimulation for 72 hr, and even at the highest E/T ratio.

To test Mϕ function, we used the cells from the peritoneal cavity. Unlike the inhibition of $CD3^+$ T-cell and $Ly49^+$ NK-cell function by CT, peritoneal Mϕ exhibited augmented function *in vitro* in response to LPS following intraperitoneal CT treatment *in vivo*. This enhanced Mϕ function after CT included increased production of nitric oxide (NO) (Fig. 3c) and of IFN-γ and IL-12p40 (Fig. 3e). These effects were mediated by Mϕ from the CT group. IT treatment following CT synergistically increased the secretory properties of Mϕ (Fig. 3c,e) and their ability to inhibit tumour cell proliferation *in vitro* (Fig. 3d). Similar functional effects to those shown in Fig. 3 were observed for peritoneal $CD11b^+$ Mϕ from mice that received intravenous CT and IT treatments (data not shown) and for mice that received their CT and IT treatments intraperitoneally. Overall, the results presented in Fig. 3 show that this CT regimen suppresses functions of T cells and NK cells but works together with IT in stimulating Mϕ functions related to anti-tumour activity.

Effect of CT and IT treatments on Mϕ phenotype

We asked investigated whether peritoneal Mϕ, unlike the splenic immune effectors (T and NK cells), might be exposed to very high concentrations of either CT drugs or anti-CD40 and CpG-ODN following intraperitoneal injection, which might affect their overall viability or function. To address this, naïve animals were transplanted with syngeneic CFSE-labelled PC and then treated with CT and IT, alone or combination, with the treatments administered either intraperitoneally or intravenously (Fig. 4). Naïve mice were injected intraperitoneally with 2×10^6 syngeneic CFSE-labelled PC obtained from naive

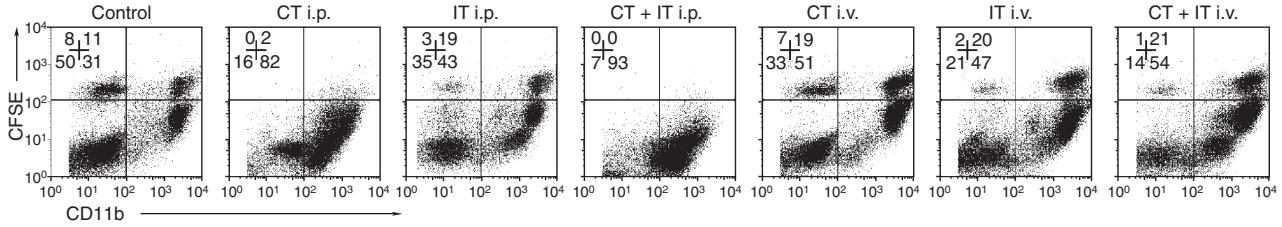

Figure 4. Route of chemotherapy (CT) and immunotherapy (IT) administration affects macrophage (Mϕ) survival and phenotype. Twenty-four hours after intraperitoneal implantation of carboxyfluoroscein succinimidyl ester (CFSE)-labelled syngeneic peritoneal cells (PC), C57BL/6 mice ($n = 3$ per group) received one cycle of CT (day 1 after PC implantation) or IT (anti-CD40 – day 4 post PC implantation followed by CpG-ODN on day 7 post PC implantation), alone or in combination, either intraperitoneally or intravenously On day 8 of the experiment, total (both resident and transplanted) PCs were harvested and tested by flow cytometry for the presence of $CFSE^+$ Mϕ. To distinguish $CFSE^+$ Mϕ from other $CFSE^+$ PC, as well as from resident $CFSE^-$ Mϕ, the total PC samples were additionally stained with anti-CD11–allophycocyanin. The numbers indicate the percentage of events in each quadrant. The data shown are representative of three experiments. i.p., intraperitoneal; i.v., intravenous.

donor mice. CT and IT, alone or in combination, were administered 24 hr after PC implantation, using the schedule described in the Materials and methods. Twenty-four hours after the last treatment (i.e. the second PBS treatment for the CT group and CpG-ODN treatment for the IT or CT+IT groups), PC were harvested and tested by flow cytometry for the presence of $CFSE^{bright}$ $CD11b^{bright}$ Mϕ (Fig. 4). These transplanted Mϕ (upper right quadrants in Fig. 4) can be easily distinguished from the resident PC Mϕ (lower right quadrants in Fig. 4) by their CFSE fluorescence signal. As shown in Fig. 4, CT but not IT, administered intraperitoneally, virtually eliminated the transplanted $CFSE^{bright}$ $CD11b^{bright}$ Mϕ. Resident Mϕ ($CFSE^{neg}$ $CD11b^+$) in mice from the group receiving intraperitoneal CT revealed an altered pattern of CD11b expression, becoming $CD11b^{dim}$ in comparison with resident Mϕ from the control group (the MFI ratio for CD11b in the $CFSE^{neg}$ $CD11b^+$ cells decreased from 761.3 in the control group to 482.1 in the intraperitoneal CT group in Fig. 4). Whether this represents a change in phenotype of the original naive resident Mϕ, or a depletion of the original resident Mϕ followed by influx of a new population with an altered phenotype, remains to be clarified. Whereas 97% of $CD11b^+$ Mϕ from mice of the control-treatment group were F4/80^{high} Gr-1^{neg}, peritoneal Mϕ from animals of the CT intraperitoneal-treatment group virtually all became F4/80^{dim} Gr-1^{high} (data not shown). In contrast to CT intraperitoneal treatment, CT administered intravenously did not affect the recovery of $CFSE^+$ $CD11b^+$ Mϕ or the pattern of CD11b expression compared with the control group (Fig. 4).

The absolute numbers of total PC and PC-derived $CD11b^+$ F4/80^+ Mϕ from mice that received CT and IT, alone or in combination, intraperitoneally or intravenously, are shown Table 1. While the intraperitoneal IT induced an increase in total PC number ($^*P \leq 0{\cdot}05$) and the intraperitoneal CT (alone or with IT) induced a decrease in recovered PC ($^{**}P \leq 0{\cdot}05$), the numbers of PC-derived $CD11b^+$ F4/80^+ Mϕ were similar for all four treatment groups and similar for intraperitoneal versus intravenous treatment.

Table 1. Quantitative changes in splenic leucocyte subsets after treatment with chemotherapy (CT) and/or immunotherapy (IT)

	Intraperitoneal		Intravenous	
	Total PC ($\times 10^6$)	$CD11b^+$ F4/80^+ Mϕ ($\times 10^6$)	Total PC ($\times 10^6$)	$CD11b^+$ F4/80^+ Mϕ ($\times 10^6$)
Control	4·5 ± 0·32	1·2 ± 0·34	4·6 ± 0·39	1·26 ± 0·35
CT	2·5 ± 0·41	1·3 ± 0·36	3·9 ± 0·31	1·48 ± 0·54
IT	8·7 ± 0·81*	1·2 ± 0·5	5·6 ± 0·42	1·4 ± 0·36
CT + IT	1·8 ± 0·18**	1·3 ± 0·4	3·7 ± 0·32	1·58 ± 0·46

Absolute numbers of total peritoneal cells (PC) and $CD11b^+$ PC from mice that received CT or IT, alone or in combination, intraperitoneally or intravenously, are shown. Results are presented as mean ± standard error of the mean (SEM) of three mice per treatment group. $^*P \leq 0{\cdot}05$; $^{**}P \leq 0{\cdot}05$ compared with the control group in that column. The data shown are representative of three experiments.

$CD11b^+$ Mϕ comprise the major population of tumour-infiltrating leucocytes

The results presented in Fig. 3a–e show that CT (alone or in combination with IT) inhibits NK and T-cell function, but enables Mϕ, in naïve non-tumour-bearing mice, to remain active and even primed to further stimulation with IT. In the next series of experiments we investigated whether CT and IT, alone or in combination, influenced the phenotype of TAM.

C57BL/6 mice bearing established subcutaneous B16 tumours, received a single intravenous cycle of CT and IT, alone or in combination, starting on day 8 after tumour

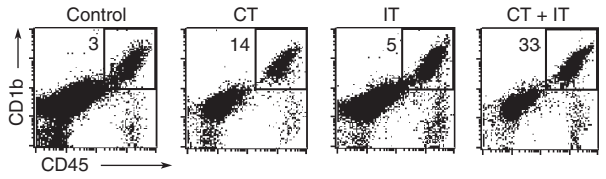

Figure 5. CD11b$^+$ macrophage (Mϕ) comprise the major population of CD45$^+$ tumour-infiltrating leucocytes (TIL) in B16 tumours. C57BL/6 mice [$n = 3$ for control, chemotherapy (CT) and immunotherapy (IT) treatment groups, $n = 6$ for the CT + IT treatment group] were injected subcutaneously with B16 cells (day 0). Mice were treated with one cycle of CT (day 8) or IT (anti-CD40 on day 11, CpG on day 14), alone or in combination. On day 15 after tumour implantation, the tumours were harvested, processed to a single-cell suspension, and viable cells were studied by flow cytometry for the prevalence of CD45$^+$ (pan-leucocyte marker)/CD11b$^+$ (pan-Mϕ marker) cells. The numbers in the right upper quadrants represent the percentage of CD45$^+$ CD11b$^+$ Mϕ (gate) in the pool of total (tumour cells + non-tumour stromal cells + TIL) viable cells. Of the total CD45$^+$ TILs, CD11b$^+$ cells comprised 89% in the control group, 95% in the CT-treatment group, 91% in the IT-treatment group and 94% in the CT + IT-treatment group.

implantation. Twenty-four hours after the last treatment (i.e. on day 15 after tumour implantation), the tumours were harvested, processed to a single-cell suspension and tested by flow cytometry for TAM in a pool of tumour-infiltrating leucocytes (TIL) by counterstaining for CD45 (pan-leucocyte marker) and CD11b (Fig. 5). The results indicate that CD11b$^+$ TAM are the major leucocyte population among CD45$^+$ TIL, and that CD11b$^+$ Mϕ comprised 89–95% of the total CD45$^+$ TIL in all treatment groups. The results also suggest that CT + IT treatment results in a relative increase in the percentage of CD11b$^+$ TAM in the tumour-derived single cell suspension compared with control cells, probably via reduction of the total number of B16 tumour cells in the preparation.

In the next experiment we analyzed the phenotype of TAM within B16 tumours from mice treated with CT, alone or in combination with IT, or with vehicles alone. The results suggest that TAM are present in two subsets – CD11b$^+$ F4/80$^+$ Gr-1^{bright} and CD11b$^+$ F4/80$^+$ Gr-1^{dim} – and that CT, administered alone or in combination with IT, and to a lesser degree IT alone, enriches CD11b$^+$ TAM for the F4/80$^+$ Gr-1^{bright} subset compared with control treatment (data not shown).

Treatment of mice with CT and IT shifts the TAM phenotype from M2 to M1

The above studies confirmed results previously obtained by others[10,11,23] of a high prevalence of TAM in growing tumours. We also demonstrated that most of these CD11b$^+$ F4/80$^+$ TAM may have a bimodal expression pattern of Gr-1 (data not shown). The F4/80$^+$ Gr-1^{bright} phenotypic profile has been associated with MDSCs.[24–26] Although *in vivo* treatment with anti-CD40 plus CpG-ODN did not result in notable changes of CD11b expression on the TAM (Fig. 5), we tested whether it would affect the expression of other surface antigens and cytokines that are characteristic for Mϕ in general and for MDSC/TAM in particular.

C57BL/6 mice, bearing established subcutaneous B16 tumours, were treated with two cycles of CT and IT, alone or in combination, beginning on day 8 after tumour implantation. Twenty-four hours after the last treatment, tumours were harvested, processed to a single-cell suspension and CD11b$^+$ F4/80$^+$ TAM were gated by flow cytometry and tested for surface expression of CD40, CD80, CD86, MHC class II antigen, CD124 (IL-4Rα) and CD274 (B7-H1) and for intracellular expression of IL-10, IL-4, IFN-γ, TNF-α and IL-12p40 (Fig. 6). As shown, CD11b$^+$ F4/80$^+$ TAM from control mice treated with vehicle alone expressed the M2 phenotype, in that they expressed high levels of surface IL-4Rα and B7-H1, and produced significant amounts of IL-10 and IL-4, but did not secrete any IFN-γ, TNF-α or IL-12. Chemotherapy resulted in the down-regulation of B7-H1 and in the up-regulation of IFN-γ. Immunotherapy down-regulated the expression of B7-H1, IL-10 and IL-4, and up-regulated the expression of CD40, CD80, CD86, MHC class II, IFN-γ, TNF-α and IL-12. When these two therapies were combined, CD11b$^+$ F4/80$^+$ TAM expressed the highest levels of CD40, CD80, CD86, MHC class II, IFN-γ, TNF-α and IL-12, and the lowest levels of IL-4Rα, B7-H1 and IL10, as well as a low level of IL-4. Thus, following the combination of CT and IT, the phenotype of Mϕ within a tumour changed from a suppressive M2 pattern to an effector M1 pattern. It is possible that this change in phenotype, from M2 to M1, for TAM following combined CT + IT treatment may play a role in the observed synergistic anti-tumour effect (Fig. 1).

Discussion

CT and IT have been considered as potentially antagonistic forms of cancer treatment because of the lymphopenia, immunosuppression and myelosuppression that can be induced by many cytotoxic drugs. This paradigm has been challenged by preclinical and clinical observations that have demonstrated therapeutic synergy between certain CT and IT regimens.[27–29] Several proposed mechanisms for CT + IT synergy include increased tumour antigen cross-presentation,[30] partial activation of antigen-presenting cells[31] and their priming to CD40-ligation,[32] tumour debulking,[33] partial sensitization of tumour cells to lysis by cytotoxic T cells,[34] reduction in function of negative regulatory cells,[35] increased access of immune cells to tumours after CT[36] and others.[37,38] In this study we describe, to our knowledge for the first

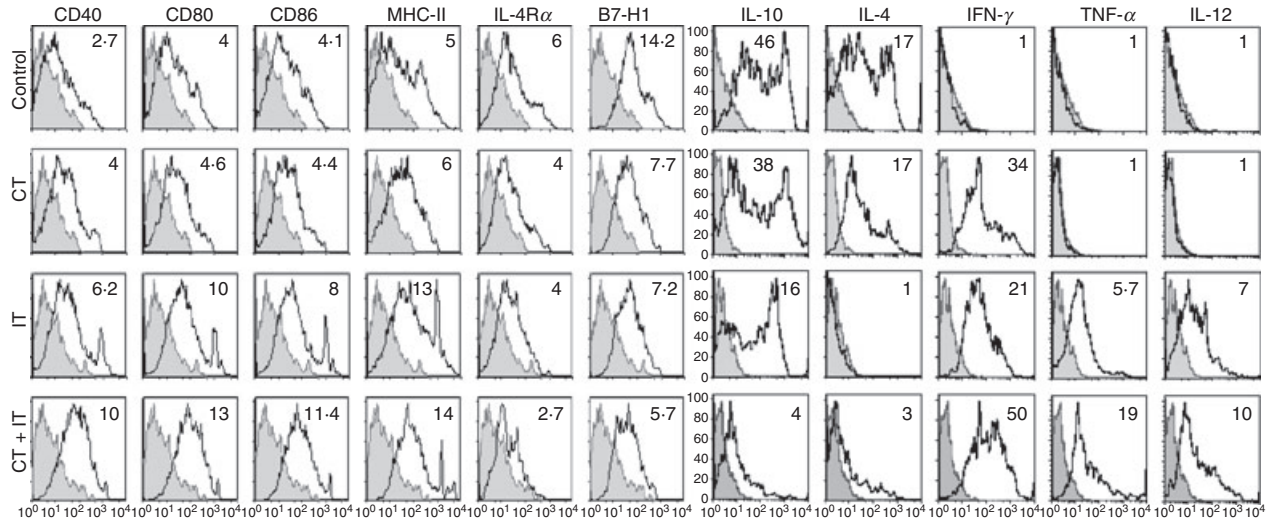

Figure 6. Chemotherapy (CT) and immunotherapy (IT) alter the phenotype and cytokine profile of tumour-associated macrophages (TAM). C57BL/6 mice ($n = 3$ for control, CT- and IT-treatment groups; $n = 6$ for the CT + IT-treatment group) bearing established subcutaneous B16 tumours were treated with two cycles of CT or IT, alone or in combination, as described in Fig. 1(c,d). One day after the last treatment [the second phosphate-buffered saline (PBS) injection for the CT-treatment group, or CpG-ODN for the IT- and the CT + IT-treatment groups], the mice were killed and the tumours were harvested and processed to a single-cell suspension. Tumour-associated cells were gated on $CD11b^+$ F4/80^+ macrophages (Mϕ) and analyzed by flow cytometry for expression of various surface antigens and intracellular cytokines (open histograms) as compared with isotype controls (shaded histograms). The mean fluorescence intensity (MFI) ratios (numbers in histograms) were computed as described in the Materials and methods. Data are representative of two separate experiments, with similar results obtained on each occasion.

time, a different mechanism of synergy between multidrug CT and IT that is based on TAM activation and their partial repolarization from Mϕ with an M2 tumour-promoting phenotype into Mϕ with an M1 anti-tumour effector phenotype.

The VCD-CT regimen is used frequently in combination with other drugs for the treatment of patients with solid and haematological malignancies. Considerable myelosuppression, neutropenia, lymphopenia and thrombocytopenia are among the most frequent side effects of this protocol. Consistent with the results of clinical reports, in our experiments a single cycle of CT resulted in some anti-tumour effects and lymphopenia with overall redistribution of major subsets of immune cells in the spleen. This CT regimen also compromised the ability of splenic T cells and NK cells to respond to stimulation via CD3 or IL-2 receptors, respectively, at least within the first 7–8 days after a single cycle of CT treatment. Taking into consideration that Mϕ are more resistant than lymphocytes to the lethal effects of certain CT,[22,39] we decided to combine CT with IT with the hope of stimulating Mϕ to induce an anti-tumour effect that would augment the anti-tumour activity of the CT. In our recent preclinical studies of IT we found that treatment with anti-CD40 and CpG-ODN induced strong activation of Mϕ that were capable of killing tumour cells *in vitro* as well as mediating anti-tumour effects *in vivo* in the absence of T cells and/or NK cells.[8,9] In this study, functional *in vitro* tests revealed that a cycle of treatment with anti-CD40 and CpG-ODN was not able to restore the CT-induced suppressed responses of T cells or NK cells. In contrast to T cells and NK cells, peritoneal Mϕ from CT-treated mice became primed to both anti-CD40 and CpG-ODN stimulation *in vivo* and to LPS stimulation *in vitro*, as measured by secretion of NO, IL-12 and IFN-γ. This Mϕ activation was associated with the statistically significant increase in the number of $CD11b^+$ splenic Mϕ in CT + IT-treated mice. *In vivo*, combined administration of CT with IT resulted in synergistic anti-tumour effects against the B16 and 9464D tumours, especially when animals received two versus just one cycle of CT + IT. In a separate study, using an intraperitoneal B16 model, we found that the anti-tumour effect of cyclophosphamide + anti-CD40 + CpG-ODN IT was reduced by Mϕ depletion with clodronate-containing liposomes, identifying Mϕ as *in vivo* anti-tumour effector cells (data not shown).

In experiments where CT and/or IT treatments were administered intraperitoneally, we investigated whether peritoneal Mϕ, unlike the splenic immune effectors, might be exposed to very high concentrations of either CT drugs or anti-CD40 and CpG-ODN following intraperitoneal injection, which might affect their overall viability or function. To address this, naïve animals were transplanted with syngeneic CFSE-labelled PC and then treated with CT and IT, alone or in combination, with the treatments administered either intraperitoneally or intravenously. PC samples from the group treated intra-

peritoneally with CT contained no CFSE-labelled donor cells [neither $CD11b^+$ PC (Mϕ) nor $CD11b^-$ PC]. This suggested that local (intraperitoneal) CT administration was toxic for the mature $CFSE^+$ donor Mϕ, resulting in their apoptosis. Interestingly, 1 day (data not shown) and even 8 days (Table 1 and Fig. 4) after a single cycle of intraperitoneal treatment, PC samples from the mice treated intraperitoneally with CT still retained relatively normal numbers of endogenous cells, the majority of which were $CD11b^{dim}$ $F4/80^{dim}$ $GR\text{-}1^{bright}$. This suggests that the CT administered intraperitoneally may be directly toxic to the mature $CD11b^+$ Mϕ (both from the donor and from the host), and that by the time the PCs are harvested, a new population of host bone marrow-derived $CD11b^{dim}$ Mϕ responsive to IT has repopulated the peritoneum. In contrast to intraperitoneal CT, intraperitoneal administration of anti-CD40 plus CpG-ODN did not affect the viability of $CFSE^+$ PC, which were readily identifiable in the pool of total PC. Indeed, in our previous studies, when naïve adherent Mϕ were exposed *in vitro* to anti-CD40 plus LPS or CpG-ODN, a sustained Mϕ activation of both secretory and cytotoxic function was documented.[8,40,41] Either treatment (CT or IT), used alone or in combination but administered intravenously, did not affect donor Mϕ viability in the peritoneum, as transplanted $CFSE^+$ Mϕ were easily detectable in samples of total PC.

Following CT, IT or CT + IT treatment, we noted the expansion of a group of PC that express intermediate amounts of CD11b (Fig. 4), which are otherwise infrequent in the pool of PC cells from control mice. These $CD11b^{dim}$ PC were also $F4/80^{dim}$ $Gr\text{-}1^{bright}$ (compared with Mϕ from control-treated mice), thereby expressing an 'immature' phenotype. Some $CD11b^{bright}$ $F4/80^{bright}$ cells in samples of PC from IT groups treated intraperitoneally, CT groups treated intravenously, IT groups treated intravenously and CT + IT groups treated intravenously, also expressed Gr-1 (data not shown). Whereas $CD11b^{dim}$ $F4/80^{dim}$ $Gr\text{-}1^{bright}$ PC cells could be immature myeloid cells that have recently migrated into the peritoneal cavity (and probably, into other compartments) from the bone marrow, the $CD11b^{bright}$ $F4/80^{bright}$ $Gr\text{-}1^{bright}$ cells could be mature, resident peritoneal Mϕ that were induced by the treatments to express Gr-1. Indeed, IT, when administered intraperitoneally, caused slight down-regulation of F4/80 and considerable up-regulation of Gr-1 on virtually all naïve Mϕ that possessed a classical 'mature' phenotype ($CD11b^{bright}$ $F4/80^{bright}$ $Gr\text{-}1^{neg}$) before implantation, and which retained that phenotype in animals that received control treatment (data not shown). Whereas down-regulation of F4/80 on mature Mϕ is known to be associated with the state of activation[42–44] and involves IFN-γ, TNF-α and other cytokines, the phenomenon of induced expression of Gr-1 on mature Mϕ merits additional analysis.

It has previously been suggested that the *RB6-8C5* clone of anti-Gr-1 may cross-react with two distinct members of the Ly6 family of proteins, namely Ly6C and Ly6G (Gr-1).[45,46] Thus, we retested the IT treatment-induced Gr-1 expression of previously Gr-1-negative $CD11b^+$ $F4/80^+$ peritoneal Mϕ by using a Ly6G-specific mAb, clone 1A8, and a Ly6C-specific mAb, clone HK1.4, and found that the majority (~85%) of $CD11b^+$ $F4/80^+$ Mϕ expressed Ly6G (Gr-1), whereas up-regulated expression of Ly6C was found only on 15–25% of IT-stimulated $CD11b^+$ $F4/80^+$ Mϕ. Importantly, Ly6G and Ly6C were co-expressed on anti-CD40 + CpG-ODN-stimulated PC Mϕ. Very little Ly6G and Ly6C were expressed on $CD11b^+$ $F4/80^+$ Mϕ from the control group (I.N. Buhtoiarov, unpublished observations). As for the mechanisms accounting for Gr-1 up-regulation, it was reported that $Ly6C^+$ $Gr\text{-}1^+$ $CD11b^+$ Mϕ can be generated *in vitro* by culturing the lineage phenotype-negative, c-kit-positive haematopoietic progenitor cells in the presence of granulocyte–macrophage colony-stimulating factor (GM-CSF), stem-cell factor (SCF) and IFN-γ.[47] Thus, it might be possible that CT and/or IT induced some of these factors, which alone or in combination could alter Ly6G/Ly6C expression on naïve Mϕ *in vivo*. This last concept might be consistent with our inability to induce Gr-1 expression on adhesion-purified $CD11b^+$ $F4/80^+$ $Gr\text{-}1^{neg}$ naïve Mϕ by stimulating them with anti-CD40 plus CpG-ODN *in vitro* (data not shown), which may reflect a necessity for exogenous (i.e. not Mϕ-derived) factors to facilitate the process of this phenotypic change.

When analyzing TAM, we found that, at least in subcutaneous B16 tumours, $CD11b^+$ Mϕ comprise the overwhelming majority of total $CD45^+$ TIL, and that both CT and IT treatments enrich tumours for these $CD11b^+$ cells. $CD11b^+$ TAM in the tumour were present in two different subsets: $F4/80^+$ $Gr\text{-}1^{bright}$ and $F4/80^+Gr\text{-}1^{dim}$ (data not shown). The pattern of F4/80 and Gr-1 co-expression by $CD11b^+$ TAM strikingly resembled the phenotypic distribution of naïve splenic $CD11b^+$ Mϕ, with a slight difference in the prevalence of these subsets. In both compartments (tumour and spleen), the therapies increased the percentage of the $CD11b^+$ $F4/80^+$ $Gr\text{-}1^{bright}$ subset and decreased the percentage of the $CD11b^+$ $F4/80^+$ $Gr\text{-}1^{dim}$ subset, without significant alteration of CD11b expression. Whether this effect was caused by the selective depletion of $CD11b^+$ $F4/80^+$ $Gr\text{-}1^{dim}$ Mϕ, or the up-regulation of Gr-1 on this subset, remains unclear. Given the observation that the number of $CD11b^+$ $F4/80^+$ Mϕ increased in the spleens of CT+IT treated mice, it seems likely that Gr-1 is up-regulated on previously $CD11b^+$ $F4/80^+$ $Gr\text{-}1^{dim}$ Mϕ by the CT + IT treatment.

$CD11b^+$ $F4/80^+$ TAM from control-treated tumour-bearing mice expressed IL-4Rα, B7-H1 and high amounts of IL-10 and IL-4. Whereas tumour-associated $CD11b^+$ $F4/80^+$ Mϕ were represented by two distinct sub-

sets, only MHC class II, IL-10 and IL-4 expression showed a bimodal pattern of distribution, with the rest of the antigens examined (Fig 6) being expressed more uniformly. CT combined with IT caused a marked decrease in expression of suppressor Mϕ-associated surface antigens (IL-4Rα and B7-H1) and cytokines (IL-4 and IL-10), and in parallel augmented the expression of CD40, CD80, CD86, MHC class II, IFN-γ, TNF-α and IL-12. Hence, after two consecutive cycles of CT + IT, $CD11b^+$ Mϕ were repolarized (at least partially) from the M2 into the M1 functional phenotype. These results also suggest that changes in expression of 'signature' phenotype antigens, such as CD11b, F4/80 and Gr-1, may have limited predictive value, as patterns of alterations of their expression did not prognostically correlate with changes of expression of other tested surface antigens or intracellular cytokines.

Whereas several mechanisms of synergy between CT and IT have been proposed, the mechanism of synergy between VCD-CT and IT with anti-CD40 and CpG-ODN remains uncharacterized and probably involves several components. CT-induced leucopenia is associated with the production of endogenous granulocyte colony-stimulating factor (G-CSF), GM-CSF and several other proinflammatory cytokines, including IL-12;[36,48,49] these might facilitate the mobilization and migration of immature myeloid cells from the bone marrow, and alter the phenotype of the resident mature Mϕ in different compartments and their priming to the subsequent CD40 and TLR9 stimulation via endogenous/autocrine IFN-γ production.[8,41] Even Mϕ with an 'immature' $CD11^{dim}$ $F4/80^{dim}$ $Gr\text{-}1^{bright}$ phenotype that appeared to have recently migrated into the peritoneum following intraperitoneal CT treatment were found to be able to respond to CD40/TLR9 stimulation *in vivo* and to LPS *in vitro*.

Previously published reports suggest that CT may synergize with IT via the selective depletion of $Gr\text{-}1^+$ suppressor cells.[50] Whereas this mechanism may be involved in augmenting T-cell-mediated anti-tumour effects, it seems less important in facilitating T-cell-independent mechanisms of tumour destruction, such as those induced by anti-CD40 plus CpG-ODN IT.[8] Indeed, we did not observe any augmented anti-tumour effects of anti-CD40 plus CpG-ODN IT in B16 melanoma-bearing mice that received concomitant treatment with anti-Gr-1 (RB6-8C5 clone) mAb to deplete $Gr\text{-}1^+$ cells.[8] It is likely that the cytotoxic mechanisms utilized by myeloid suppressor $Gr\text{-}1^+$ cells to suppress T-cell immunity,[51,52] such as NO and IFN-γ, can also be involved in tumour cell destruction, especially when tumours are weakly immunogenic and cytotoxic T-cell-mediated mechanisms are not elicited. In agreement with that, we previously showed that the anti-tumour effects of anti-CD40-activated Mϕ do not require T cells and involve IFN-γ[41] and NO.[21] The results of this study further demonstrate that clinically relevant, multidrug CT, although immunosuppressive for T cells and NK cells, can synergize with Mϕ-activating IT via the repolarization of TAM and the induction of Mϕ-mediated anti-tumour effects.

Acknowledgements

This work was supported by The National Institutes of Health Grants CA87025 and CA032685 (to PMS), grants from the Midwest Athletes Against Childhood Cancer Fund (to PMS, ALR and INB), and the grant from the UW Cure Kids Cancer Coalition (INB and PMS). The authors thank Drs Jacquelyn A. Hank and Jacek Gan of The University of Wisconsin for helpful discussions. INB is a UICC fellow.

Disclosures

I.B. designed/conducted experiments, analyzed data and wrote the manuscript; P.S. and A.R. directed the project, interpreted results and helped to write and revise the manuscript; J.W. developed and provided a crucial mouse model; T.B., E.Y. and D.M. assisted with experiments.

References

1 Borella L, Green AA, Webster RG. Immunologic rebound after cessation of long-term chemotherapy in acute leukemia. *Blood* 1972; **40**:42–51.
2 Lanfranchi A, Andolina M, Tettoni K, Porta F, Locatelli F, De Manzini A, Candotti F, Albertini A. Functional depletion of T cells by vincristine and methylprednisolone as an in vitro model for the prevention of graft versus host disease. *Haematologica* 1992; **77**:11–5.
3 Multhoff G, Botzler C, Allenbacher A, Issels R. Effects of ifosfamide on immunocompetent effector cells. *Cancer Immunol Immunother* 1996; **42**:251–4.
4 Ferraro C, Quemeneur L, Prigent AF, Taverne C, Revillard JP, Bonnefoy-Berard N. Anthracyclines trigger apoptosis of both G0-G1 and cycling peripheral blood lymphocytes and induce massive deletion of mature T and B cells. *Cancer Res* 2000; **60**: 1901–7.
5 Kimhi O, Drucker L, Neumann A *et al.* Fluorouracil induces apoptosis and surface molecule modulation of peripheral blood leukocytes. *Clin Lab Haematol* 2004; **26**:327–33.
6 Mozaffari F, Lindemalm C, Choudhury A *et al.* NK-cell and T-cell functions in patients with breast cancer: effects of surgery and adjuvant chemo- and radiotherapy. *Br J Cancer* 2007; **97**:105–11.
7 Kuppner MC, Bleifuss E, Noessner E, Mocikat R, Hesler C, Mayerhofer C, Issels RD. Differential effects of ifosfamide on dendritic cell-mediated stimulation of T cell interleukin-2 production, natural killer cell cytotoxicity and interferon-gamma production. *Clin Exp Immunol* 2008; **153**:429–38.
8 Buhtoiarov IN, Lum HD, Berke G, Sondel PM, Rakhmilevich AL. Synergistic activation of macrophages via CD40 and TLR9 results in T cell independent antitumor effects. *J Immunol* 2006; **176**:309–18.
9 Wu QL, Buhtoiarov IN, Sondel PM, Rakhmilevich AL, Ranheim EA. Tumoricidal effects of activated macrophages in a mouse model of chronic lymphocytic leukemia. *J Immunol* 2009; **182**:6771–8.
10 Barrera CN, Mazzolli AB, Bustuoabad OD, Andreetta AM, Pasqualini CD. Macrophages and tumor growth. II. Cell kinetics at the site of allogeneic tumor growth. *Cancer Invest* 1985; **3**:7–13.
11 Allavena P, Sica A, Garlanda C, Mantovani A. The Yin-Yang of tumor-associated macrophages in neoplastic progression and immune surveillance. *Immunol Rev* 2008; **222**:155–61.
12 De Campos ES, Menasce LP, Radford J, Harris M, Thatcher N. Metastatic carcinoma of uncertain primary site: a retrospective review of 57 patients treated with vincristine, doxorubicin, cyclophosphamide (VAC) or VAC alternating with cisplatin and etoposide (VAC/PE). *Cancer* 1994; **73**:470–5.

13 Arndt CA, Nascimento AG, Schroeder G *et al.* Treatment of intermediate risk rhabdomyosarcoma and undifferentiated sarcoma with alternating cycles of vincristine/doxorubicin/cyclophosphamide and etoposide/ifosfamide. *Eur J Cancer* 1998; **34**:1224–9.

14 Kushner BH, Meyers PA. How effective is dose-intensive/myeloablative therapy against Ewing's sarcoma/primitive neuroectodermal tumor metastatic to bone or bone marrow? The Memorial Sloan-Kettering experience and a literature review *J Clin Oncol* 2001; **19**:870–80.

15 Solomayer EF, Feuerer M, Bai L *et al.* Influence of adjuvant hormone therapy and chemotherapy on the immune system analyzed in the bone marrow of patients with breast cancer. *Clin Cancer Res* 2003; **9**:174–80.

16 Norris MD, Burkhart CA, Marshall GM, Weiss WA, Haber M. Expression of N-myc and MRP genes and their relationship to N-myc gene dosage and tumor formation in a murine neuroblastoma model. *Med Pediatr Oncol* 2000; **35**:585–9.

17 Salcedo R, Stauffer JK, Lincoln E *et al.* IL-27 mediates complete regression of orthotopic primary and metastatic murine neuroblastoma tumors: role for CD8+ T cells. *J Immunol* 2004; **173**:7170–82.

18 Mohammad RM, Wall NR, Dutcher JA, Al-Katib AM. The addition of bryostatin 1 to cyclophosphamide, doxorubicin, vincristine, and prednisone (CHOP) chemotherapy improves response in a CHOP-resistant human diffuse large cell lymphoma xenograft model. *Clin Cancer Res* 2000; **6**:4950–6.

19 Neal ZC, Yang JC, Rakhmilevich AL *et al.* Enhanced activity of hu14.18-IL2 immunocytokine against murine NXS2 neuroblastoma when combined with interleukin 2 therapy. *Clin Cancer Res* 2004; **10**:4839–47.

20 Buhtoiarov IN, Rakhmilevich AL, Lanier LL, Ranheim EA, Sondel PM. Naive mouse macrophages become activated following recognition of L5178Y lymphoma cells via concurrent ligation of CD40, NKG2D, and CD18 molecules. *J Immunol* 2009; **182**:1940–53.

21 Lum HD, Buhtoiarov IN, Schmidt BE, Berke G, Paulnock DM, Sondel PM, Rakhmilevich AL. Tumoristatic effects of anti-CD40 mAb-activated macrophages involve nitric oxide and tumour necrosis factor-alpha. *Immunology* 2006; **118**:261–70.

22 Wheeler HR, Geczy CL. Induction of macrophage procoagulant expression by cisplatin, daunorubicin and doxorubicin. *Int J Cancer* 1990; **46**:626–32.

23 Evans R, Lawler EM. Macrophage content and immunogenicity of C57BL/6J and BALB/cByJ methylcholanthrene-induced sarcomas. *Int J Cancer* 1980; **26**:831–5.

24 Kusmartsev S, Gabrilovich DI. STAT1 signaling regulates tumor-associated macrophage-mediated T cell deletion. *J Immunol* 2005; **174**:4880–91.

25 Gabrilovich DI, Nagaraj S. Myeloid-derived suppressor cells as regulators of the immune system. *Nat Rev Immunol* 2009; **9**:162–74.

26 Ostrand-Rosenberg S, Sinha P. Myeloid-derived suppressor cells: linking inflammation and cancer. *J Immunol* 2009; **182**:4499–506.

27 Buzaid AC, Grimm EA, Ali-Osman F *et al.* Mechanism of the anti-tumour effect of biochemotherapy in melanoma: preliminary results. *Melanoma Res* 1994; **4**:327–30.

28 Soulié P, Ruffié P, Trandafir L *et al.* Combined systemic chemoimmunotherapy in advanced diffuse malignant mesothelioma. Report of a phase I-II study of weekly cisplatin/interferon alfa-2a. *J Clin Oncol* 1996; **14**:878–85.

29 Grimm EA, Smid CM, Lee JJ, Tseng CH, Eton O, Buzaid AC. Unexpected cytokines in serum of malignant melanoma patients during sequential biochemotherapy. *Clin Cancer Res* 2000; **6**:3895–903.

30 Salem ML, Díaz-Montero CM, Al-Khami AA, El-Naggar SA, Naga O, Montero AJ, Khafagy A, Cole DJ. Recovery from cyclophosphamide-induced lymphopenia results in expansion of immature dendritic cells which can mediate enhanced prime-boost vaccination antitumor responses in vivo when stimulated with the TLR3 agonist poly(I:C). *J Immunol* 2009; **182**:2030–40.

31 Nowak AK, Lake RA, Marzo AL, Scott B, Heath WR, Collins EJ, Frelinger JA, Robinson BW. Induction of tumor cell apoptosis in vivo increases tumor antigen cross-presentation, cross-priming rather than cross-tolerizing host tumor-specific CD8 T cells. *J Immunol* 2003; **170**:4905–13.

32 Nowak AK, Robinson BW, Lake RA. Synergy between chemotherapy and immunotherapy in the treatment of established murine solid tumors. *Cancer Res* 2003; **63**: 4490–6.

33 Lundy J, Lovett EJ, Hinchliffe D, Schor M. Chemoimmunotherapy of a murine fibrosarcoma: critical factors for success of combined modality therapy. *J Surg Oncol* 1977; **9**:339–45.

34 Yang S, Haluska FG. Treatment of melanoma with 5-fluorouracil or dacarbazine in vitro sensitizes cells to antigen-specific CTL lysis through perforin/granzyme- and Fas-mediated pathways. *J Immunol* 2004; **172**:4599–608.

35 Polak L, Turk JL. Reversal of immunological tolerance by cyclophosphamide through inhibition of suppressor cell activity. *Nature* 1974; **249**:654–6.

36 Bracci L, Moschella F, Sestili P *et al.* Cyclophosphamide enhances the antitumor efficacy of adoptively transferred immune cells through the induction of cytokine expression, B-cell and T-cell homeostatic proliferation, and specific tumor infiltration. *Clin Cancer Res* 2007; **13**:644–53.

37 Dudley ME, Wunderlich JR, Robbins PF *et al.* Cancer regression and autoimmunity in patients after clonal repopulation with antitumor lymphocytes. *Science* 2002; **298**:850–4.

38 Kaech SM, Tan JT, Wherry EJ, Konieczny BT, Surh CD, Ahmed R. Selective expression of the interleukin 7 receptor identifies effector CD8 T cells that give rise to long-lived memory cells. *Nat Immunol* 2003; **4**:1191–8.

39 Ibe S, Qin Z, Schüler T, Preiss S, Blankenstein T. Tumor rejection by disturbing tumor stroma cell interactions. *J Exp Med* 2001; **194**:1549–59.

40 Buhtoiarov IN, Sondel PM, Eickhoff JC, Rakhmilevich AL. Macrophages are essential for antitumour effects against weakly immunogenic murine tumours induced by class B CpG-oligodeoxynucleotides. *Immunology* 2007; **120**:412–23.

41 Buhtoiarov IN, Lum H, Berke G, Paulnock DM, Sondel PM, Rakhmilevich AL. CD40 ligation activates murine macrophages via an IFN-gamma-dependent mechanism resulting in tumor cell destruction in vitro. *J Immunol* 2005; **174**:6013–22.

42 Ezekowitz R, Alan B, Gordon S. Down-regulation of mannosyl receptor-mediated endocytosis and antigen F4/80 in Bacillus Calmette-Guerin-activated mouse macrophages. *J Exp Med* 1982; **155**:1623–37.

43 Benedict CA, De Trez C, Schneider K, Ha S, Patterson G, Ware CF. Specific Remodeling of Splenic Architecture by Cytomegalovirus. *PLoS Pathog* 2006; **2**:0164–73.

44 Menson EN, Wilson RA. Lung-phase immunity to Schistosorna rnansoni: definition of alveolar macrophage phenotypes after vaccination and challenge of mice. *Parasite Immunol* 1990; **12**:353–66.

45 Fleming TJ, Fleming ML, Malek TR. Selective expression of Ly-6G on myeloid lineage cells in mouse bone marrow. RB6-8C5 mAb to granulocyte-differentiation antigen (Gr-1) detects members of the Ly-6 family. *J Immunol* 1993; **151**:2399–408.

46 Nagendra S, Schlueter AJ. Absence of cross-reactivity between murine Ly-6C and Ly-6G. *Cytometry* 2004; **58**:195–200.

47 Ferret-Bernard S, Saï P, Bach JM. In vitro induction of inhibitory macrophage differentiation by granulocyte-macrophage colony-stimulating factor, stem cell factor and interferon-gamma from lineage phenotypes-negative c-kit-positive murine hematopoietic progenitor cells. *Immunol Lett* 2004; **91**:221–7.

48 Bruserud O, Foss B, Petersen H. Hematopoietic growth factors in patients receiving intensive chemotherapy for malignant disorders: studies of granulocyte-colony stimulating factor (G-CSF), granulocyte-macrophage colony stimulating factor (GM-CSF), interleukin-3 (IL-3) and Flt-3 ligand (Flt3L). *Eur Cytokine Netw* 2001; **12**:231–8.

49 Banning U, Mauz-Körholz C, Muhammad Q *et al.* Endogenous pro-inflammatory cytokines in children and adolescents during chemotherapy-induced neutropenia. *Pediatr Hematol Oncol* 2002; **19**:561–8.

50 Suzuki E, Kapoor V, Jassar AS, Kaiser LR, Albelda SM. Gemcitabine selectively eliminates splenic Gr-1+/CD11b+ myeloid suppressor cells in tumor-bearing animals and enhances antitumor immune activity. *Clin Cancer Res* 2005; **11**:6713–21.

51 Movahedi K, Guilliams M, Van den Bossche J, Van den Bergh R, Gysemans C, Beschin A, De Baetselier P, Van Ginderachter JA. Identification of discrete tumor-induced myeloid-derived suppressor cell subpopulations with distinct T cell-suppressive activity. *Blood* 2008; **111**:4233–44.

52 Watanabe S, Deguchi K, Zheng R, Tamai H, Wang LX, Cohen PA, Shu S. Tumor-induced CD11b+Gr-1+ myeloid cells suppress T cell sensitization in tumor-draining lymph nodes. *J Immunol* 2008; **181**:3291–300.